



**HAL**  
open science

## Shvo-Type Metal-Ligand Cooperative Catalysts: Tethered $\eta(5)$ -Oxocyclohexadienyl Ruthenium Complexes

Emmanuel Puig, Raphaël Verron, Manel Kéchaou-Perrot, Laure Vendier,  
Heinz Gornitzka, Karinne Miqueu, Jean-Marc Sotiropoulos, Cedric  
Fischmeister, Pierre Sutra, Alain Igau

► **To cite this version:**

Emmanuel Puig, Raphaël Verron, Manel Kéchaou-Perrot, Laure Vendier, Heinz Gornitzka, et al.. Shvo-Type Metal-Ligand Cooperative Catalysts: Tethered  $\eta(5)$ -Oxocyclohexadienyl Ruthenium Complexes. *Organometallics*, 2022, 41 (11), pp.1391-1402. 10.1021/acs.organomet.2c00123 . hal-03715383

**HAL Id: hal-03715383**

**<https://hal.science/hal-03715383v1>**

Submitted on 9 Oct 2022

**HAL** is a multi-disciplinary open access archive for the deposit and dissemination of scientific research documents, whether they are published or not. The documents may come from teaching and research institutions in France or abroad, or from public or private research centers.

L'archive ouverte pluridisciplinaire **HAL**, est destinée au dépôt et à la diffusion de documents scientifiques de niveau recherche, publiés ou non, émanant des établissements d'enseignement et de recherche français ou étrangers, des laboratoires publics ou privés.

# Shvo-type Metal-Ligand Cooperative Catalysts : Tethered $\eta^5$ -Oxocyclohexadienyl Ruthenium Complexes

Emmanuel Puig<sup>a,b</sup>, Raphaël Verron<sup>c</sup>, Manel Kechaou-Perrot<sup>a,b,†</sup>, Laure Vendier<sup>a,b</sup>, Heinz Gornitzka<sup>a,b</sup>, Karinne Miqueu<sup>d</sup>, Jean-Marc Sotiropoulos<sup>d</sup>, Cédric Fischmeister<sup>\*,c</sup>, Pierre Sutra<sup>a,b</sup> and Alain Igau<sup>\*,a,b</sup>

<sup>a</sup> CNRS, LCC (Laboratoire de Chimie de Coordination), 205 route de Narbonne, BP 44099, F-31077 Toulouse Cedex 4, France. E-mail : alain.igau@lcc-toulouse.fr

<sup>b</sup> Université de Toulouse, UPS, INPT, F-31077 Toulouse Cedex 4, France.

<sup>c</sup> Univ Rennes, CNRS, ISCR (Institut des Sciences Chimiques de Rennes) – UMR 6226 F-35042 Rennes, France.

<sup>d</sup> CNRS/Université de Pau & des Pays de l'Adour, E2S-UPPA, Institut des Sciences Analytiques et de Physico-Chimie pour l'Environnement et les Matériaux (IPREM), UMR CNRS 5254, 2 avenue du Président P. Angot, 64053 Pau, Cedex 09, France.

**KEYWORDS:** *tethered metal complexes, piano-stool complexes, metal-ligand cooperativity, bifunctional catalysis, transfer hydrogenation catalysis, formic acid, base free additive.*

---

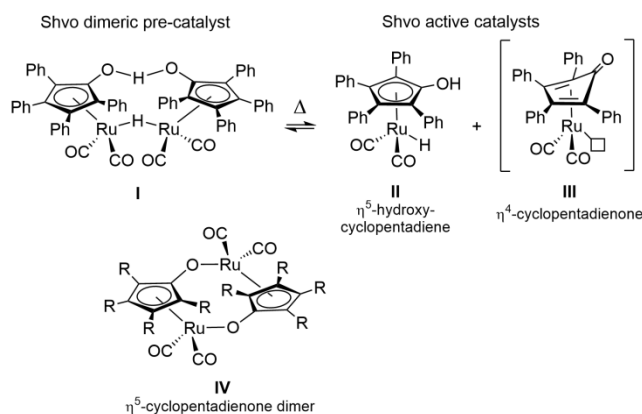
**ABSTRACT:** Diverse synthetic routes of tethered  $\eta^5$ -oxocyclohexadienyl ruthenium complexes, which are the extended version of the  $\eta^4$ -cyclopentadienone Shvo-type active catalyst, are described and their reactivity studies are reported. An original dimeric  $\eta^5$ -oxocyclohexadienyl compound has been isolated and its solid state structure was established by X-ray analysis. DFT computational data suggested that this dimeric compound is prone to generate a coordinatively unsaturated mononuclear Lewis acid metal complex bearing a Lewis basic  $\pi$ -coordinated  $\eta^5$ -oxocyclohexadienyl ligand. Preliminary studies in (transfer)hydrogenation of acetophenone confirmed that the dimeric  $\eta^5$ -oxocyclohexadienyl complex behaves as a bifunctional catalyst with metal-ligand cooperativity. Promising results were obtained under base-free conditions using dihydrogen, *i*PrOH and formic acid as hydrogen donors, the later being active in water hence highlighting the robustness and stability of the catalyst and opening perspectives toward sustainable catalytic transformations.

---

## INTRODUCTION

Metal–ligand cooperativity in molecular catalysts has been demonstrated to be an efficient strategy for a large number of chemical transformations.<sup>1</sup> Shvo dimeric pre-catalyst **I**,<sup>2</sup> one of the earliest complex which has initiated the large development of the metal-ligand cooperation concept, is the prototypical example in the family of half sandwich (or piano-stool) transition metal complexes.<sup>3</sup> Shvo type-catalysts have shown high catalytic activity in hydrogenation reactions and have led to explosive growth of their application.<sup>4</sup> Since its preparation, Shvo dimeric pre-catalyst **I** is believed to dissociate in solution into two species, the hydride  $[(\eta^5\text{-C}_5\text{Ph}_4\text{OH})\text{Ru}(\text{H})(\text{CO})_2]$  (**II**) and the coordinatively unsaturated  $\eta^4$ -cyclopentadienone complex  $[(\eta^4\text{-C}_5\text{Ph}_4\text{O})\text{Ru}(\text{CO})_2]$  (**III**) (Chart 1).<sup>2,4</sup> Complex **II** could not be crystallized; however, the available NMR data are consistent with the proposed structure. The 16-electron monomolecular entity **III** has never been observed to date and a recent combined experimental/computational study envisage the possibility that **III** is not viable in the typical experimental conditions of catalytic reactions.<sup>5</sup> Note that the corresponding dimer complex **IV** was independently prepared and structurally characterized.<sup>6</sup> Surprisingly, dimer **IV** species (Chart 1), which can be considered as precursors of the corresponding active coordinatively unsaturated  $\eta^4$ -cyclopentadienone mononuclear complexes of the type **III**, have been little investigated in catalysis.<sup>7</sup>

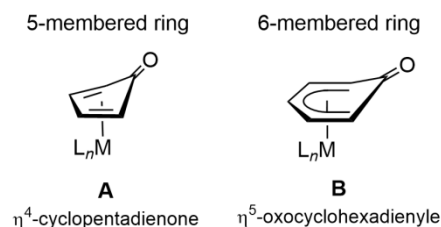
**Chart 1.** Representation of the Shvo dimeric pre-catalyst **I** and its thermal dissociation products **II** and **III**, and dimeric  $\eta^5$ -cyclopentadienone complex **IV**.



By analogy with the 5-membered ring  $\eta^4$ -cyclopentadienone complexes **A**, of which the Shvo active catalyst **III** is the archetypical model, we assume that the 6-membered ring homologues, the  $\eta^5$ -oxocyclohexadienyl metal complexes **B**, may be of interest in metal-ligand cooperative bifunctional

catalysis (Chart 2). The synthesis of piano-stool  $\eta^5$ -oxocyclohexadienyl transition metal complexes B can be achieved via different chemical pathways which allow to tune the steric and electronic properties of the  $\pi$ -coordinated phenoxy ring as well as the other ligands grafted on the metal center. Examples of such type of  $\eta^5$ -oxocyclohexadienyl complexes have been described in the literature from group 6 to group 10 transition metal elements.<sup>8</sup> In the area of  $\pi$ -coordinated arene organometallic chemistry, particular attention has been devoted to the development of arene-tethered complexes<sup>9</sup> in an attempt to improve the stability of the corresponding species and to increase stereocontrol at the metal center of chiral catalysts. Surprisingly, before our studies<sup>10</sup> no-tethered  $\eta^5$ -oxocyclohexadienyl metal complexes were reported. Moreover, even though the first  $\eta^5$ -oxocyclohexadienyl metal complex,  $[(\eta^5\text{-OC}_6\text{H}_5)\text{Ru}(\text{H})(\text{PPh}_3)_2]$  was published in 1976 by Cole-Hamilton, Young and Wilkinson,<sup>11</sup> these species, incorporating an arene ligand with acido-basic properties, have been totally ignored from potential applications in a number of domains such as homogeneous catalysis.

**Chart 2.** General representation of half-sandwich  $\eta^4$ -cyclopentadienone A and  $\eta^5$ -oxocyclohexadienyl B transition metal complexes.



Prototypical catalytic reactions involving transition metal complexes with acido-basic ligands are reduction reactions. Reduction reactions are ubiquitous in organic synthesis and despite their undeniable benefit compared to conventional stoichiometric reductants such as metal-hydrides, these catalytic reduction processes still require basic co-catalyst(s). This matter of fact is problematic for environmental and economic impact concerns and it is also an issue considering the limitations imposed by these basic conditions as these processes cannot be applied to substrates containing base-sensitive functional groups. For these reasons, the development of base-free reduction processes is of high interest and has received a lot of attention. Considering catalysts without preformed metal-hydride species,<sup>12</sup> reduction reactions using isopropanol as “hydrogen donor” are intensively studied.<sup>13</sup> In this case, metal-ligand cooperation is generally at play and involves acido-basic properties of the ligand. Base-free hydrogenation of ketones with

dihydrogen is much less developed. It has been originally described by Noyori and Okhuma<sup>14</sup> and more recently, several groups have reported the base free hydrogenation using either preformed metal-hydride complexes<sup>15</sup> or cooperating ligands.<sup>16</sup> Finally, the base free hydrogenation of ketones employing formic acid as hydrogen donor as only been rarely reported since the original report by Watanabe in the early 80's.<sup>17</sup> Very recently, a Shvo-type molybdenum complex was reported for the base-free reduction of aldehydes, ketones and amines<sup>18</sup> while an iridium<sup>19</sup> and a ruthenium<sup>20</sup> complex were briefly reported for the reduction of acetophenone. Interestingly, few results on the additive-free hydrogenation and transfer hydrogenation of levulinic acid into  $\gamma$ -valerolactone have been recently reported.<sup>21</sup>

Herein, we present sequential and straightforward synthetical routes for the preparation of tethered  $\eta^5$ -oxocyclohexadienyl half-sandwich ruthenium(II) complexes with an emphasis on a combined experimental and theoretical study on an unprecedented dimeric  $\pi$ -coordinated phenoxy entity. Considering the structure of this  $\eta^6:\kappa^1$ -P  $\pi$ -coordinated phenoxy *O*-bridged ruthenium dimer, determined by X-ray crystal analysis, preliminary catalytic tests in hydrogenation reaction for the reduction of acetophenone and a diarylaldimine are presented. Moreover, efficient transfer hydrogenation reactions conducted with formic acid as hydrogen donor in base-free condition are reported.

## RESULTS AND DISCUSSION

### Synthesis of tethered $\eta^5$ -oxocyclohexadienyl complexes

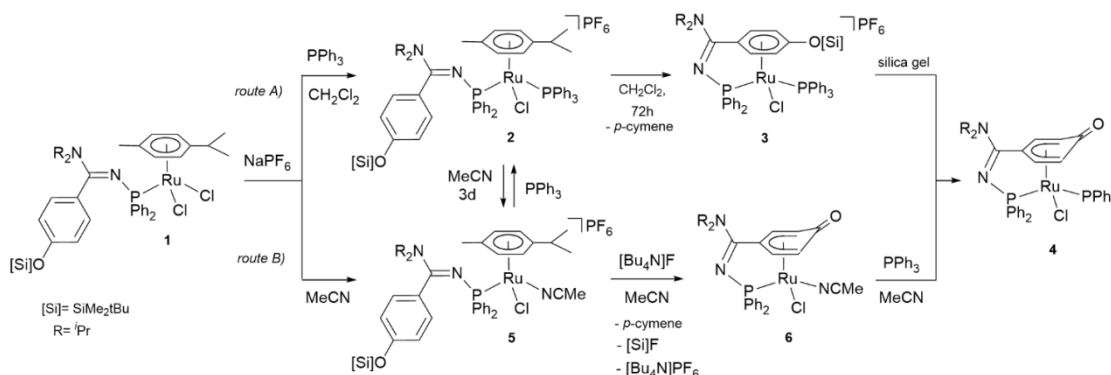
Mechanistic preconceptions suggested that the tethered  $\eta^5$ -oxocyclohexadienyl ruthenium complex **4** could be prepared independently *via* the two alternative routes shown in Scheme 1 and this expectation was readily confirmed. Starting from the linear amidino phosphine complex **1**, to prepare complex **4**, route A) involves the formation of the tethered  $\eta^6$ -silyloxyarene complex **3**; and route B) goes through the acetonitrile solvate tethered  $\eta^5$ -oxocyclohexadienyl complex **6**.

As shown in Scheme 1, route A), complex **1** was reacted in dichloromethane at room temperature with 1 equiv. of NaPF<sub>6</sub> in the presence of PPh<sub>3</sub> to form quantitatively the linear arene complex **2** identified by <sup>31</sup>P NMR as two doublets resonances ( $J_{PP} = 50.8$  Hz) at 42.8 (large, PN) and 23.5 (PPh<sub>3</sub>) ppm. Treatment of the crude reaction mixture gave compound **2** in 80% purity along with the presence of another growing derivative **3**. When the reaction mixture was stirred for 72 h, complex **2** totally disappeared to give the monomeric tethered  $\eta^6$ -silyloxyarene complex **3** isolated in pure form as an orange powder in 70% yield after column chromatography under basic conditions. This compound **3** exhibits two doublets resonances at 70.3 (PN) and 36.0 (PPh<sub>3</sub>) ppm in the <sup>31</sup>P{<sup>1</sup>H} NMR spectrum ( $J_{PP} = 49.4$  Hz). When **3** was passed

through a column of silica gel, the monomeric tethered  $\eta^5$ -oxocyclohexadienyl complex **4** was formed in 40% isolated yield.

We developed an other synthetical pathway (Scheme 1, route *B*) to prepare **4** in acetonitrile which involves the addition of  $\text{NaPF}_6$  on **1** to give quantitatively the corresponding linear amidino phosphine solvate complex **5** which showed a large signal at  $\delta^{31}\text{P}$  50.0 ppm. Cleavage of the Si-O bond was easily achieved with TBAF; removal of the *p*-cymene arene ligand was observed and the corresponding mononuclear tethered solvate  $\eta^5$ -oxocyclohexadienyl complex **6** was formed quantitatively according to  $^{31}\text{P}$  NMR ( $\delta^{31}\text{P}$  77 ppm). Starting from the latter solvate product **6**, after addition of  $\text{PPh}_3$ , complex **4** is obtained in 70% isolated yield. It is worth noting that depending on the experimental conditions compounds **2** and **5** interconvert (Scheme 1). If compound **2** is solubilized in acetonitrile, total conversion to compound **5** is observed after 3 days at room temperature. Starting from **5**, addition of  $\text{PPh}_3$  in  $\text{CH}_2\text{Cl}_2$  led instantaneously to the complete formation of **2**.

**Scheme 1.** Sequential synthesis of the tethered  $\eta^5$ -oxocyclohexadienyl ruthenium complex **4** via route A) and B) starting from the linear phosphamidine precursor **1**.

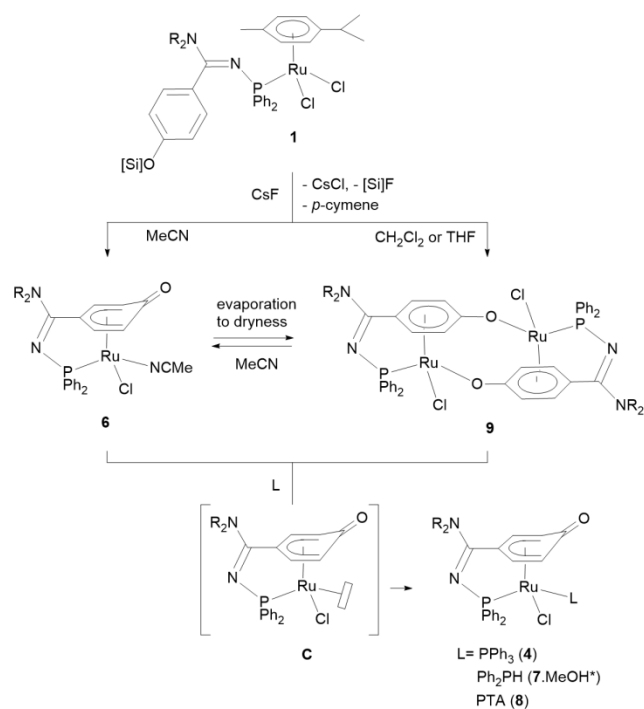


We demonstrated that following the synthetical strategy described in route *B*, it was possible to process simultaneously on complex **1** to the chloride abstraction and the Si-O bond cleavage using  $\text{CsF}$  as the unique reagent to obtain quantitatively in solution the acetonitrile complex **6** in a straightforward way (Scheme 2).<sup>10</sup> If dichloromethane or THF is used instead of acetonitrile, addition of  $\text{CsF}$  on **1** led to the formation of a thermally and air stable new tethered species **9** (Scheme 2) which is isolated as an orange powder in more than 80% yield. It exhibits a singlet signal at 76 ppm in  $^{31}\text{P}$  NMR. DOSY NMR experiment revealed a diffusion coefficient in  $\text{CD}_2\text{Cl}_2$  for **9** significantly lower compared to the one registered for the mononuclear  $\eta^5$ -oxocyclohexadienyl species **4** which is favorable with the formation of a dimeric structure for **9**. When the latter **9** was dissolved in  $\text{CD}_3\text{CN}$ , formation of the monomolecular

solvate complex **6** was observed and confirmed by NMR analysis. Interestingly, in CD<sub>3</sub>CN, the diffusion coefficient of **6** is higher compared to complex **4** (see SI, Figure S7). Moreover, when the acetonitrile solution of the  $\eta^5$ -oxocyclohexadienyl solvate complex **6** is evaporated to dryness, according to IR and solid state NMR experiments, the resulting powder corresponds to the dimeric compound **9** (Scheme 2). Its structure has been confirmed by a solid X-ray crystal analysis (see section X-ray diffraction studies of complexes **9-14**). It is noteworthy that complexes **6** and **9** are formal precursors for the formation of the coordinatively unsaturated 16-electron  $\eta^5$ -oxocyclohexadienyl complex **C** (Scheme 2, Figures 1 & 3) incorporating in its structure a Lewis basic oxygen site and an acidic vacant metal coordination site. These peculiar features, encountered in Shvo catalyst, are at the origin of metal-ligand cooperation and make complex **C** a valuable bifunctional catalyst candidate.

Chelation of the cyclic fragment of the amidino phosphine ligand on the ruthenium atom is accompanied by a deshielded effect on the <sup>31</sup>P chemical shift of about 30 ppm. All proton and carbon atoms of the  $\pi$ -coordinated ligand in tethered complexes **3,4** and **6-9** have been identified and display their own resonances in accord with the stereogenic nature of the metal center. As well as for compound **4**, the low frequency shift of the four  $\eta^5$ -C<sub>6</sub>H<sub>4</sub>O-ring protons in **3,4** and **6-9** compared to **1**, **2**, and **5** indicates  $\pi$ -coordination to the ruthenium center. In the <sup>13</sup>C NMR spectrum, six resonances were observed for the  $\eta^5$ -oxocyclohexadienyl unit, one deshielded singlet at 159 ppm corresponding to the carbon atom linked to the oxygen atom, and five shielded signals corresponding to the other carbon atoms of the ligand in the range of those found for **4**.

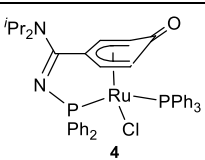
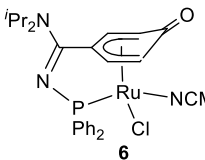
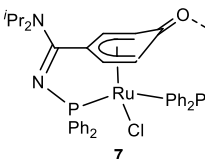
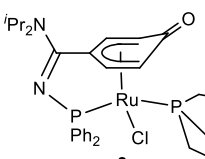
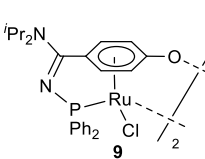
**Scheme 2.** Synthesis of the dimeric  $\pi$ -coordinated phenoxy complex **9** and monomeric tethered  $\eta^5$ -oxo-cyclohexadienyl entities **4** and **6-8**.



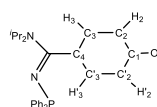
As it is often observed with  $\eta^5$ -oxocyclohexadienyl cyclic ligand, in complex **7**, formation of an adduct through hydrogen bonding with residual methanol coming from the purification process occurred which explain the slight shielded effect on the  $\delta^{13}\text{C}$  (CO) at 156 ppm compared to the other identified  $\eta^5$ -oxocyclohexadienyl complexes **4**, **6** and **8** (Table 1). Note that the  $^{13}\text{C}$  NMR chemical shift of the C=N carbon atom of the backbone amidino organophosphorus ligand in **1-9** complexes in the region of 163 to 166 ppm is not perturbed by the chelating coordination mode.



**Table 1.** NMR data of tethered half-sandwich  $\eta^5$ -oxocyclohexadienyl 4 and 6-8 and dimer 9 complexes.

| Complexes   | $^{31}\text{P}$                     | $^{13}\text{C}$ NMR ( $J_{\text{CP}}$ ) |                |                 |                |                |                | $^1\text{H}$ NMR ( $^3J_{\text{HH}}$ ) |               |               |                 |
|---|-------------------------------------|---|----------------|-----------------|----------------|----------------|----------------|--|---------------|---------------|-----------------|
|   | NMR<br>( $J_{\text{PP}}$ ) $^\circ$ | C1                                      | C2             | C3              | C4             | C3'            | C2'            | H2                                     | H3            | H3'           | H2'             |
|    | 73,38<br>(44)                       | 159.1                                   | 85.3<br>(6.2)  | 101.1<br>(6.7)  | 112.0<br>(5.1) | 88.2           | 79.1<br>(5.1)  | 4.94<br>(7.1)                          | 5.98<br>(7.1) | 4.27<br>(6.5) | 3.67<br>(6.5)   |
|    | 77                                  | 160.7                                   | 83.8<br>(2.4)  | 86.9<br>(5.6)   | 106.3          | 89.9<br>(6.6)  | 73.1<br>(14.3) | 4.59<br>(6.7)                          | 5.21<br>(6.7) | 5.44<br>(6.6) | 4.62<br>(6.6)   |
|    | 74,34<br>(53)                       | 156.2                                   | 94.8<br>(9.3)  | 102.5<br>(7.5)  | 105.7<br>(7.5) | 85.5           | 74.9<br>(10.3) | 5.55<br>(7.2)                          | 5.90<br>(7.2) | 4.84<br>(6.0) | 4.35<br>(broad) |
|   | 79,-<br>34<br>(46)                  | 159.2                                   | 87.8<br>(9.2)  | 104.2<br>(10.3) | 110.0<br>(9.2) | 84.0           | 73.1<br>(10.9) | 5.19<br>(6.9)                          | 5.92<br>(6.9) | 5.11<br>(5.1) | 4.74<br>(5.1)   |
|  | 76                                  | 164.7                                   | 80.3<br>(14.2) | 72.7<br>(3.2)   | 106.3<br>(7.5) | 83.17<br>(4.8) | 83.9<br>(2.3)  | 5.67<br>(5.7)                          | 4.90<br>(5.7) | 5.26<br>(6.3) | 6.89<br>(6.3)   |

Numbering scheme of the phenoxy



ring :

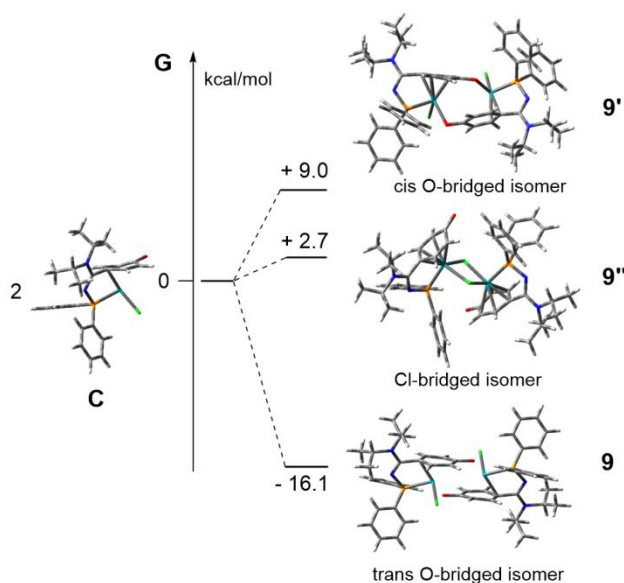
## Computational Studies

We turned to DFT calculations to get deeper insight on the structural and electronic features of the  $\pi$ -coordinated phenoxy dimer **9** which is a potential precursor of the coordinatively unsaturated 16-electron  $\eta^5$ -oxocyclohexadienyl complex C. Let us point out that a careful analysis of the potential energy surface (PES), reveals the presence of 3 isomers for the dimeric product which correspond to the  $\eta^6$ : $\kappa^1$ -P O-bridged  $\pi$ -coordinated phenoxy isomers with Cl atoms in trans and cis position (**9** and **9'** respectively) and the Cl-bridged isomer (**9''**). As shown in Figure 1, calculation of the dimerization energy from C

evidences a thermodynamic preference for the formation of the trans-O-bridged isomer **9** ( $\Delta G$  : -16.1 kcal/mol), which is consistent with its solid state characterization recorded by X-ray diffraction analysis (see X-ray Diffraction Studies section). Dimer **9** is calculated to be the global minimum. Isomer **9'** was found to be higher in energy ( $\Delta G$  : 9.0 kcal/mol) and **9''** lies at 18.8 kcal/mol above **9**.

Experimentally, at room temperature, when the dimeric complex **9** is solubilized in MeCN, formation of the corresponding mononuclear  $\eta^5$ -oxocyclohexadienyl solvate complex **6** is observed (Scheme 2). In contrast, in THF, the corresponding tethered mononuclear solvate  $[(\eta^5\text{-OC}_6\text{H}_4\text{-C}(\text{N}^i\text{Pr}_2)=\text{NPh}_2)\text{Ru}(\text{THF})\text{Cl}]$  **6'** complex is not formed, the structure of the initial dimeric complex **9** remains. These results are consistent with the computed dissociation energies. The formation of **6'** from **C** in THF is an endergonic reaction ( $\Delta G_{\text{THF}}$  : +3.3 kcal/mol). On the contrary, the formation of **6** from **C** in acetonitrile is exergonic ( $\Delta G_{\text{MeCN}}$  : -9.6 kcal/mol), in agreement with the identification of **6** in MeCN solution. Interestingly, dimer **9** is recovered from **6** after evaporation of the acetonitrile solution (Scheme 2). This “dimerization” process of **6** into **9** is a thermodynamically favorable conversion ( $\Delta G$  : -13.5 kcal/mol). Therefore, we may reasonably envisage that starting from **6** removal of MeCN solution induce the transient formation of the 16-electron coordinatively unsaturated complex **C** to give the dimeric product **9**.

**Figure 1.** Relative stability ( $\Delta G$  in kcal/mol) of the 3 isomers associated to the  $\eta^6:\kappa^1$ -P *O*-bridged dimeric  $\pi$ -coordinated phenoxy forms (**9** and **9'**) and the dimeric Cl-bridged form (**9''**).



In order to have a better insight on the nature of the ligands around the metal in complexes **C**, **4**, **6**, **6'** and **9**, NBO analysis was performed. The distribution of the NPA charges on the  $\pi$ -coordinated cyclic fragment of the tethered ligand in the dimer **9** and in the monomers **C**, **4**, and **6** were examined. Interestingly, we noticed that the respective values of the charges on each of the carbon atoms C(1)-C(6) which form the 6-membered ring and the charge on the oxygen atom do not differ significantly for all the complexes cited above whatever it is a dimeric or a mononuclear complex. Analysis of the charge transfer from the THF, MeCN and PPh<sub>3</sub> ligands to the metallic fragment **C** indicate a stronger donation in **4**, than in **6** and than in **6'** (CT : 0.70, 0.20, 0.17 respectively). For complex **4** a  $\sigma_{\text{RuIP}}$  bond has been found whereas in complex **6** and **6'** a strong donor acceptor interaction ( $n_{\text{N}}$  or  $n_{\text{O}} \rightarrow d(\text{Ru})$ ) has been identified at the second order perturbation theory, with a stabilizing interaction  $\Delta E(2)$  at 120 kcal/mol in **6** and 47 kcal/mol in **6'**. Moreover, the Natural Localized Molecular orbital associated to the Ligand  $\rightarrow$  Ru interaction evidences an increase of the participation of the Ru atom going from **4** to **6** and **6'** (34.5%, 16.6% and 7.0% respectively), in agreement with the electronic donor ability of the corresponding L ligand.

Considering the structural data of the  $\pi$ -coordinated phenoxy ring, the bond lengths between C-C atoms are comparatively similar in the dimer **9** and in the  $\eta^5$ -oxocyclohexadienyl monomers **C**, **4**, and **6**. However, by examining the Ru(1)-C(1) bond lengths, we found that this distance is longer in compounds **4** and **C** than those computed in dimer **9** (~2.492 Å for **9** to 2.572 and 2.641 Å for **4** and **C** respectively). For dimer **9**, the geometrical considerations support - as shown by the solid XRD analysis - an  $\eta^6$ -hapto  $\pi$ -coordination type. Moreover, if we compare the Wiberg Bond Indices (WBI), and in particular the index relative to the C(1)-O(1) bond, we note that the value calculated for dimer **9** (~1.2) is lower compared to the value computed for mononuclear **4**, **6** and **C** complexes (~1.6). The latter is in favor for a double bond C-O character and consequently in agreement with a delocalization on the 5 carbon centers characteristic of the  $\eta^5$ -coordination mode in a  $\pi$ -coordinated oxocyclohexadienyl cyclic fragment.

### Chemical reactivity of $\eta^5$ -oxocyclohexadienyl complexes

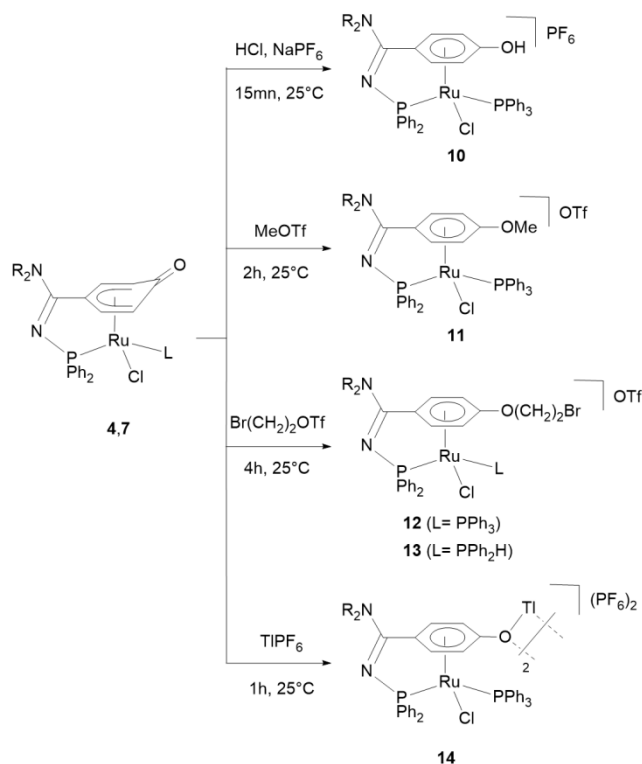
The reactivity of  $\eta^5$ -oxocyclohexadienyl complexes towards Brønsted acids, electrophiles, thallium salt and dihydrogen was investigated in order to comfort the potential interest of these complexes in catalysis.

Interconversion of  $\eta^5$ -oxocyclohexadienyl transition metal complexes to their corresponding phenol compounds, upon protonation/deprotonation processes, has been largely exemplified in the literature. In a first approach, a stoichiometric amount of HCl was added at room temperature on the  $\eta^5$ -oxocyclohexadienyl entity **4**. After 15 min., quantitative formation of the expected phenol complex **10** was observed and this complex was isolated in 90% yield after anion exchange with NaPF<sub>6</sub> (Scheme 3).

The phenol compound **10** exhibits in the  $^{31}\text{P}\{^1\text{H}\}$  NMR spectrum two doublets resonances at 70.2 (PN) and 29.8 (PPh<sub>3</sub>) ppm with a  $J_{\text{PP}} = 52.0$  Hz along with the sextuplet of the PF<sub>6</sub> counter anion centered at -144.7 ppm. In  $^1\text{H}$  NMR, variable temperature experiments did not allow us to observe the phenolic proton. However, we were able to obtain X-ray quality single-crystals of **10** to confirm its phenolic structure and demonstrate the basic character of the  $\eta^5$ -oxocyclohexadienyl ligand (see x-ray diffraction studies section). Note that all attempts to isolate the corresponding phenol products formed after addition of HX (X= Cl, OTf) on complexes **6** and **9** were unsuccessful. Broad signals by  $^{31}\text{P}$  NMR were observed in the region of 78 to 84 ppm depending on the solvent of the reaction and the concentration of the solution; these chemical shifts may be attributed to the expected phenol complexes in dynamic intermolecular interactions. All these products decompose in a multitude of  $^{31}\text{P}$  NMR signals along the course of the different treatment processes attempted to isolate them.

Very few reactions have been investigated to test the nucleophilicity of the  $\eta^5$ -oxocyclohexadienyl ligand. In this aim, electrophiles have been reacted with complexes **4** and **7**. Addition of the alkylating agent MeOTf on **4** led to the quantitative formation of the corresponding  $\eta^6$ -methoxybenzene chelate complex **11** (Scheme 3). Note that the use of MeI did not form **11** but gave selectively the iodine analogue complex of **4**, [ $(\eta^5\text{-OC}_6\text{H}_4\text{-C}(\text{N}^i\text{Pr}_2)=\text{NPPh}_2)\text{Ru}(\text{PPh}_3)\text{I}$ ] **4'**. Interestingly, when 2-bromoethyl triflate was reacted with **4**, quantitative formation of the  $\eta^6$ -bromoethoxybenzene complex **12** was observed. An identical reaction was conducted with the  $\eta^5$ -oxocyclohexadienyl complex **7** incorporating the functionalized PH-phosphine; the same selectivity was observed and the product **13** was isolated in good yield. Chlorine abstraction was not observed after addition of TIPF<sub>6</sub> on **4**; instead of that, the  $\eta^6$ -phenoxy thallium complex **14** was isolated as a dimeric species in its solid form.

**Scheme 3.** Reactivity of tethered  $\eta^5$ -oxocyclohexadienyl complexes **4** and **7**.

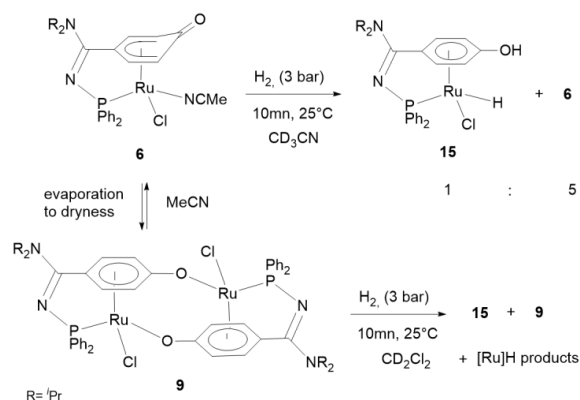


The  $^{31}\text{P}$  chemical shift of the phosphorus atom of the tethered ligand in complexes **11-14** in the range of 70 ppm as well as their  $J_{\text{PP}}$  coupling constant, are in the same range as those registered for the  $\eta^5$ -oxocyclohexadienyl complexes **4, 6-8**. In accord with the stereogenic nature of the metal center, all proton and carbon atoms of the  $\pi$ -coordinated ligand in tethered complexes display their own resonances. In  $^1\text{H}$  NMR, the low frequency shift of the four  $\eta^5$ - $\text{C}_6\text{H}_4\text{O}$ -ring protons in **11-14** complexes indicates  $\pi$ -coordination to the ruthenium center. In the  $^{13}\text{C}$  NMR spectrum, the chemical shift for complexes **10-12** of the carbon atom linked to the oxygen atom is in the range of 137-138 ppm which is typical for those found in  $\eta^6$ -coordinated alkyl phenoxy ether complexes. Interestingly, the singlet observed at 151.5 ppm for the C(1)-O(1) bond in complex **13** is in between those registered for  $\eta^5$ -oxocyclohexadienyl complexes **4, 6-8** and  $\eta^6$ -coordinated alkyl phenoxy ether complexes **11-14**. Note that the  $^{13}\text{C}$  NMR chemical shift of the C=N carbon atom of the backbone amidino organophosphorus ligand in **11-14** complexes in

the region of 163-164 ppm is not perturbed by the  $\eta^6$ -coordinated phenoxy ligand. These results clearly evidenced the nucleophilic character of the phenoxy ligand.

Finally, the reactivity of complexes **6** and **9** under dihydrogen atmosphere was monitored by NMR. These complexes are precursors of **C** (Scheme 2 & Fig 1) which should split  $H_2$  leading to the protonation of the phenoxy ligand with concomitant formation of a ruthenium-hydride to form the corresponding phenol hydride complex **15** (Scheme 4). The reactivity of the solvate **6** toward  $H_2$  was investigated by exposing a  $CD_3CN$  solution of **6** to 3 bar of  $H_2$  at room temperature in an NMR tube. After 10 min the clean formation of a new product at  $\delta^{31}P$  89 ppm in a 1:5 ratio relative to the starting complex was observed.  $^1H$  revealed the presence of an hydride chemical shift at  $\delta^1H$  -9.30 with a  $^2J_{HP}$  coupling constant of 42 Hz and a broad protonic phenol signal centered at 10.9 ppm. All these NMR data recorded in solution for this compound are in favor of the formation of the expected  $\pi$ -coordinated phenol hydride complex **15** which is stable for 3 days in solution. Under the same experimental conditions, dimer **9** in  $CD_2Cl_2$  led to the formation of the phenol hydride product **15** along with the presence of the starting complex **9** and other non-identified products with hydride signals recorded from -7 to -14 ppm. The ability of complexes **6** and **9** to split dihydrogen into a ruthenium hydride species bearing an acidic phenolic proton confirms the potential of such complexes for catalytic applications, in particular in reduction catalysis.

**Scheme 4.** Hydrogenation reaction of tethered  $\eta^5$ -oxo-cyclohexadienyl monomeric **6** and dimeric **9** complexes.



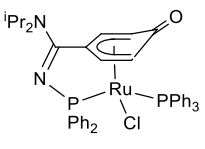
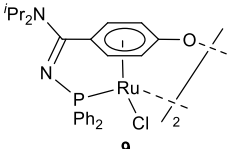
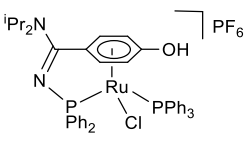
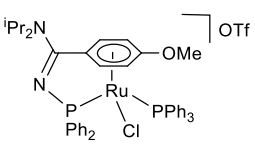
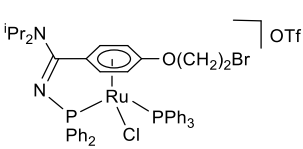
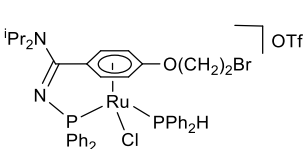
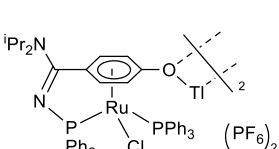
Finally, monomeric **6** and dimeric **9** complexes have been reacted with formic acid (FA) which is one of the privileged hydrogen donor source in transfer hydrogenation catalysis because of its unique properties, including among others, easy transportation, handling and favorable energy density.<sup>22</sup> At RT in MeCN after 12h, addition of FA (3 eq.) on monomer **6** resulted in the total consumption of the starting compound and in the presence of  $CO_2$  ( $\delta^{13}C$  125 ppm) and the formation of a major compound with a  $^{31}P$

chemical shift at 128 ppm which was not possible to identify. Note that we were not able to observe in the reaction mixture by  $^1\text{H}$  NMR any metal hydride products. When the dimeric complex **9** was reacted with FA (10 eq.) in  $\text{CH}_2\text{Cl}_2$ , after 12 h at RT, we detected the same products as those observed in the reaction with the monomeric solvate complex **6** and no hydride compounds were observed as well. However, when the same reaction was conducted with **9** in DMSO,<sup>23</sup> Ru-H hydride compounds were detected as a broad  $^{31}\text{P}$  NMR chemical shift at 84 ppm and hydride signals at -10.0 and -11.6 ppm with a  $J_{\text{HP}}$  of 30 and 32 Hz, respectively. An other hydride complex was detected at 127 ppm and -10.5 ppm in  $^{31}\text{P}$  and  $^1\text{H}$  NMR, respectively, with a  $J_{\text{HP}}$  of 31 Hz. Unfortunately we were not able to identify those complexes. It is worthy to mention that two other hydrido compounds were observed at -11.5 ppm and -14.4 ppm without  $J_{\text{HP}}$  coupling constant. In view of the results recorded with FA, we could anticipate that FA will act as an hydrogen donor source in transfer hydrogenation catalysis in the presence of the dimeric complex **9**.

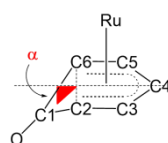
### X-ray Diffraction Studies of Complexes **4**, **9-14**

Solid state X-ray structures studies are pertinent to assign the bonding mode of  $\pi$ -coordinated 6-membered aryloxy ring type ligands, whether it is an  $\eta^5$ - or  $\eta^6$ -bonding mode. The solid molecular structures of compounds **4**<sup>10</sup>, **9-14**<sup>24</sup> have been determined by X-ray analysis. It is noteworthy to remind that the most striking structural features observed for the  $\eta^5$ -oxocyclohexadienyl derivatives, among the other representative structural features, are the following : a) the carbon-carbon distances are shorter in the 'pentadienyl' fragment of the ring than in the bonds to C(1), b) the C(1)-O(1) bond is tilted above the plane formed by the pentadienyl fragment C(2)-C(6), and has substantial double-bond character which ranges from 1.23 to 1.25 Å,<sup>25</sup> c) puckering of the ring is identified by the rather long Ru(1)-C(1) bond distance. These effects, observed in **4** (Table 2), are not so pronounced for  $\eta^6$ -bonding mode though these complexes also show some degree of non-planarity, as well as variation in the internal C-C distances and angles.

**Table 2.** X-Ray crystallographic data of tethered  $\eta^5$ -oxocyclohexadienyl/ $\eta^6$ -bound phenoxy rings complexes 4, 9-14.

| Complexes  | C(1)-<br>O(1) | C(1)-<br>C(2) | C(1)-<br>C(6) | C(2)-<br>C(3) | C(3)-<br>C(4) | C(4)-<br>C(5) | C(5)-<br>C(6) | $\alpha$ ( $^\circ$ ) | Ru(1)-<br>C(1) | Ru(1)-<br>C(4) |
|--|---------------|---------------|---------------|---------------|---------------|---------------|---------------|-----------------------|----------------|----------------|
|  <p style="text-align: center;"><b>4</b></p>    | 1.246         | 1.467         | 1.438         | 1.382         | 1.421         | 1.417         | 1.420         | 8.78                  | 2.672          | 2.164          |
|  <p style="text-align: center;"><b>9</b></p>    | 1.301         | 1.457         | 1.396         | 1.393         | 1.441         | 1.403         | 1.437         | /                     | 2.409          | 2.101          |
|  <p style="text-align: center;"><b>10</b></p>   | 1.344         | 1.427         | 1.399         | 1.407         | 1.430         | 1.406         | 1.428         | /                     | 2.378          | 2.180          |
|  <p style="text-align: center;"><b>11</b></p>  | 1.344         | 1.394         | 1.435         | 1.427         | 1.411         | 1.434         | 1.395         | /                     | 2.398          | 2.137          |
|  <p style="text-align: center;"><b>12</b></p> | 1.350         | 1.400         | 1.426         | 1.420         | 1.405         | 1.438         | 1.381         | /                     | 2.542          | 2.253          |
|  <p style="text-align: center;"><b>13</b></p> | 1.362         | 1.422         | 1.387         | 1.393         | 1.435         | 1.410         | 1.431         | /                     | 2.380          | 2.160          |
|  <p style="text-align: center;"><b>14</b></p> | 1.279         | 1.455         | 1.434         | 1.392         | 1.438         | 1.417         | 1.429         | /                     | 2.460          | 2.128          |

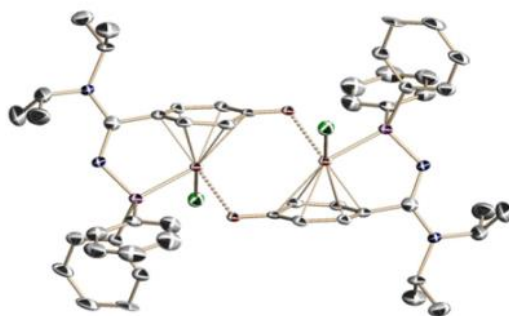
Numbering scheme of the phenoxy ring :





After several attempts, we were successful to obtain good quality single-crystals of **9** for X-ray diffraction analysis. The ORTEP diagram is presented in Figure 2. The solid-state structure confirmed the proposed dimeric nature of compound **9** in which the phenolate-type ring is  $\pi$ -coordinated to the ruthenium and *O*-bridged to the second ruthenium fragment thus achieving an 18-electron configuration. Each ruthenium atom bears a chlorine atom and the tethered backbone  $\kappa^1$ -phosphino amidine  $\pi$ -coordinated arene ligand. All six C(1)–C(6) carbon atoms and the oxygen atom of the phenolate-type arene unit - C<sub>6</sub>H<sub>4</sub>O in **9** are coplanar. In comparison to the true  $\eta^5$ -bonding mode of phenolate-type ring in **4** (C(1)–O(1) 1.246 Å), the C(1)–O(1) bond of 1.301 Å in **9** is elongated and is in between of those registered for  $\eta^5$ -C<sub>6</sub>H<sub>5</sub>O oxocyclohexadienyl<sup>9,13</sup> and  $\eta^6$ -C<sub>6</sub>H<sub>5</sub>OR alkyl phenoxy<sup>26</sup> transition metal complexes (Table 2). Note that the Ru(1)–O(1) bond distances of 2.115 Å in the bridging interactions of the dimeric species **9** are comparable to what is observed in the two solid state structures of the homologous dimeric 5-membered ring transition metal complexes of type **IV** [2.137<sup>6a</sup> and 2.117<sup>6b</sup> Å] described so far in the literature in which the  $\pi$ -coordinated cyclopentadienyl rings with the oxygens bound to the second ruthenium. The bond lengths and angles values in the *N*-phosphino amidine backbone <sup>i</sup>Pr<sub>2</sub>N–C=N–PPh<sub>2</sub> in **9** are comparable to those recorded for the corresponding tethered  $\eta^6$ -arene- $\kappa^1$ -*P*-ruthenium complexes previously described by us.<sup>16</sup>

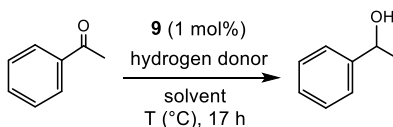
**Figure 2.** Solid state structure of dimer **9**. Thermal ellipsoids are depicted at the 50% probability level. H-atoms have been omitted for clarity. Selected bond distances (Å) and bond angles (deg): C(1)–O(1).303(7); Ru(1)–O(1) 2.115(4); C(1)–O(1)–Ru(1) 120.1(3).



Intra-ring C–C bond distances and Ru–C bond lengths compare well with a benzene type ligand coordinated to a ruthenium atom. All these structural features in the solid state provide evidence that the  $\pi$ -bonded phenolate-type ligands in dimeric species **9** possesses  $\eta^6$ -arene character.<sup>10g,14,27</sup> The solid state X-ray structure studies of complexes **10-14** show the six membered rings to have the carbon atoms C(1)–C(6) and the oxygen atoms nearly in the same plane. The  $\pi$ -benzene binding mode of the six membered ring ligand is indicated by the C–C bonds distances (1.381–1.455 Å). The C(1)–O(1) bond length of 1.34–1.36 Å for **10-13** is consistent with a single-bond character and comparable to analogous distances previously reported for  $\pi$ -coordinated phenol<sup>28</sup> and alkyl phenoxy<sup>29</sup> piano-stool ruthenium complexes. In the case of the dimeric compound **14**, the relatively short C(1)–O(1) bond distance (1.28 Å) is in the range of those already reported for such type of dimeric thallium derivatives and is attributed to a partial delocalization of the negative charge on the oxygen atom on the phenolate-type ring.<sup>30</sup> Note that the bond lengths and angles in the *N*-phosphino amidine backbone  $^i\text{Pr}_2\text{N}-\text{C}=\text{N}-\text{PPh}_2$  in **9-14** are comparable to those recorded for the corresponding tethered  $\eta^6$ -arene- $\kappa^1$ -P-ruthenium complexes previously described by us.<sup>31</sup> The general structural features of the arene ligand are largely in favor for an  $\eta^6$ -coordinated nature of the 6-membered ring.

### Hydrogenation and Transfer Hydrogenation Catalysis with dimer **9**

The reactivity of tethered  $\eta^5$ -oxocyclohexadienyl ruthenium complexes with Brønsted acids, electrophiles, and dihydrogen was investigated and confirm the potential interest of these complexes in catalysis. It was calculated that the thermal dissociation of dimer **9** into the mononuclear coordinatively unsaturated 16-electron tethered  $\eta^5$ -oxocyclohexadienyl complex **C** is a low-energy. Considering the structure of this species **C** which possesses acido-basic properties homologous to the Shvo active catalyst **III**, we anticipated that the dimeric compound **9** is the ideal precursor for catalytic applications.

**Table 3.** Reduction of acetophenone catalyzed by **9** using various hydrogen donors<sup>a</sup>.

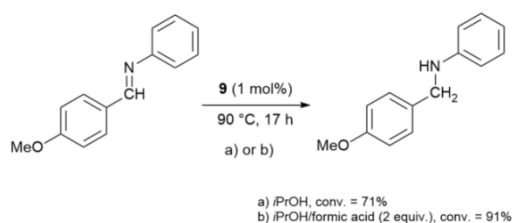
| Entry | Hydro-<br>gen<br>donor | T<br>(°C) | Sol-<br>vent     | Conver-<br>sion<br>(%) <sup>b</sup> |
|-------|------------------------|-----------|------------------|-------------------------------------|
| 1     | H <sub>2</sub>         | (60 75    | To-              | 23                                  |
| 2     | H <sub>2</sub>         | (60 90    | To-              | 59                                  |
| 3     | H <sub>2</sub>         | (30 90    | <i>i</i> PrOH    | 99 (99) <sup>c</sup>                |
| 4     | <i>i</i> PrOH          | 90        | <i>i</i> PrOH    | 33                                  |
| 5     | HCOOH                  | 75        | <i>i</i> PrOH    | 48 (46) <sup>c</sup>                |
| 6     | HCOOH                  | 75        | H <sub>2</sub> O | 50                                  |
| 7     | HCOOH                  | 90        | <i>i</i> PrOH    | 58                                  |
| 8     | HCOOH                  | 90        | H <sub>2</sub> O | 72                                  |

[a] Acetophenone (0.857 mmol, 100  $\mu$ L), **9** (1 mol%, 9.3 mg), Solvent (1.0-1.5 mL), 17 h. [b] Determined by <sup>1</sup>H NMR. [c] With Shvo catalyst.

Then, we decided to investigate the potential metal-ligand cooperation of **C** in the base-free reduction of acetophenone. As depicted in Table 2, hydrogenation of acetophenone with the dimeric pre-catalyst **9** proceeded smoothly under 60 bar of dihydrogen in toluene (Table 3, entries 1, 2) but 99 % conversion was reached in *i*PrOH under 30 bar of dihydrogen which is identical to the Shvo catalyst (Table 3, entry 3). The reaction performed under transfer condition in isopropanol was much more sluggish reaching a modest 33% conversion after 17 h at 90 °C (Table 2, entry 4). Considering the actual state of the art, the most remarkable results were achieved under hydrogen transfer conditions using formic acid as hydrogen donors (Table 3, entries 5-8). Under these conditions valuable conversion was reached at 75 °C both in *i*PrOH and H<sub>2</sub>O as solvent and could be substantially improved upon heating at 90 °C (72% conversion, Table 2, entry 8). Here again, the performance of the catalyst was found similar to the Shvo

catalyst (Table 3, entry 5). Preliminary studies indicate that this reaction proceeds predominantly by dehydrogenation/hydrogenation rather than true transfer hydrogenation as conversions dropped significantly when the reactions were conducted in an open vessel.

**Scheme 5.** Reduction of an imine catalyzed by **9** (conversion determined by  $^1\text{H}$  NMR).



The catalytic activity was further evidenced with the reduction of an imine-containing substrate (Scheme 5).<sup>32</sup> Here again, **9** proved competent for the efficient reduction of the imine substrate in particular using a mixture of *i*PrOH and FA as hydrogen donors in the absence of base.

In light of recent studies in homogeneous transfer hydrogenation reaction with metal-ligand cooperative catalysts,<sup>5b</sup> mechanistic proposal will require further experimental and theoretical studies to understand more precisely the catalytic activity and improve the catalyst's performances.

## CONCLUSION

Through this study, we evidenced two independent pathways for the synthesis of the tethered  $\eta^5$ -oxocyclohexadienyl metal complex **4**. We extended the preparation of  $\eta^5$ -oxocyclohexadienyl metal complexes to the PH-functionalized **7** and water soluble **8** compounds using a straightforward synthetic strategy. We have isolated a thermally and air stable tethered species **9**. Its dimeric solid state structure was determined by X-ray diffraction analysis and revealed an original  $\pi$ -coordinated  $\eta^6$ -phenolate-type ring *O*-bridged to the other metal center. DFT computational data suggested that the dimeric entity **9** is prone to generate a mononuclear 16-electron  $\eta^5$ -oxocyclohexadienyl metal complex **C** with a vacant coordination site on the Lewis acid metal center and a Lewis basic pendant  $\pi$ -coordinated phenolate-type ligand. This theoretical observation has been confirmed by the quantitative formation of the  $\eta^5$ -oxocyclohexadienyl solvate metal complex **6** from **9** in acetonitrile solution.

The reactivity of  $\eta^5$ -oxocyclohexadienyl complexes towards Brønsted acids and electrophiles emphasized the basicity and nucleophilicity of the oxygen atom of the phenolate-type ligand. The reactivity under dihydrogen atmosphere of complexes **6** and **9**, precursors of the transient 16-electron  $\eta^5$ -oxocyclohexadienyl complex **C**, was monitored by NMR and showed the splitting of H<sub>2</sub> to form the corresponding phenol hydride complex **15**. These results confirm the potential interest of such complexes for catalytic applications in particular in reduction catalysis.

With all the experimental and theoretical informations on  $\eta^5$ -oxocyclohexadienyl complexes in hands, we have tested the dimeric ruthenium complex **9** in base-free hydrogenation and transfer hydrogenation catalysis conditions. Among other results registered in this study, we demonstrated that **9** operates in water with formic acid as the hydrogen source without base additive. It is reasonable to propose that the dimeric species precursor **9** acts as the 16-electron mononuclear ruthenium active species **C** which behaves as a bifunctional metal-ligand cooperative catalyst. The precatalyst **9** was also competent for the reduction of an imine substrate under base free conditions.

Preliminary results showed that dimer **9** has comparable catalytic performances than the Shvo catalyst **I**. The two alternative routes to prepare  $\eta^5$ -oxocyclohexadienyl ruthenium complexes via a stepwise process (Scheme 1) are investigated in the group for the preparation of a series of new complexes for which the first and second coordination sphere of the metal will be readily modified in the aim to enhance the performance of the corresponding catalysts.

We are also presently expanding the scope of ketone and imine hydrogenation reaction, as well as studying its mechanistic implications. Although the reactivity of **9** has been well established and some catalytic hydride intermediates identified, at this stage, it remains hypothetical to propose a reliable catalytic mechanism.<sup>5b,33</sup>

In order to improve the catalytic activity of our systems, the synthesis of new families of dimeric  $\pi$ -coordinated phenolate-type species are currently under investigation in our laboratory. Incorporation of first row metal center are envisaged as well as the preparation of their optically active version for asymmetric catalysis.

## **AUTHOR INFORMATION**

### **Corresponding Author**

\*E-mail for A.I.: alain.igau@lcc-toulouse.fr

\*E-mail for C.F.: cedric.fischmeister@univ-rennes1.fr

## **Present Address**

† Total Exploration Production, CSTJF, Avenue Larribau, 64018 Pau Cedex – FRANCE

## **Author Contributions**

Methodology, investigation and validation: Emmanuel Puig, Pierre Sutra and Alain Igau (organometallic synthesis); Raphael Verron and Cédric Fischmeister (catalytic studies); Heinz Gornitzka and Laure Vendier (X-ray diffraction); Karinne Miqueu and Jean-Marc Sotiropoulos, (DFT calculation). Project administration, conceptualization, supervision: Alain Igau. Writing original draft: Cédric Fischmeister and Alain Igau. Resources and funding acquisition: Raphael Verron and Emmanuel Puig.

## **Notes**

The authors declare no competing financial interest.

## **ACKNOWLEDGMENTS**

M.K. is grateful to MESR for a doctoral fellowship. C.D., P.S. and A.I. thank the ANR for financial support, as well as E.P. and R.V. are grateful respectively for post-doctoral and Ph.D fellowships (Project CatEngy ANR-18-CE07-0006-01). Dr. Y. Coppel and C. Bijani are acknowledged for their help in NMR analysis. The “Direction du Numérique” of the Université de Pau et des Pays de l’Adour, MCIA (Mésocentre de Calcul Intensif Aquitain) and CINES under allocation A009080045 made by Grand Equipement National de Calcul Intensif (GENCI) are acknowledged for computational facilities.

## REFERENCES

- (1) Selected reviews: a) Noyori R.; Ohkuma, T. Asymmetric Catalysis by Architectural and Functional Molecular Engineering: Practical Chemo- and Stereoselective Hydrogenation of Ketones. *Angew. Chem., Int. Ed.* **2001**, *40*, 40–73; b) Clapham, S. E.; Hadzovic, A.; Morris, R. H. Mechanisms of the H<sub>2</sub>-hydrogenation and transfer hydrogenation of polar bonds catalyzed by ruthenium hydride complexes. *Coord. Chem. Rev.* **2004**, *248*, 2201–2237; c) Grützmacher, H. Cooperating Ligands in Catalysis. *Angew. Chem., Int. Ed.* **2008**, *47*, 1814–1818; d) Gunanathan, C.; Milstein, D. Metal-ligand cooperation by aromatization-dearomatization: a new paradigm in bond activation and "green" catalysis. *Acc. Chem. Res.*, **2011**, *44*, 588–602; e) O. Eisenstein, Crabtree, R. H. Outer sphere hydrogenation catalysis. *New J. Chem.* **2013**, *37*, 21–27; f) Zhao, B.; Han, Z.; Ding, K. The N–H Functional Group in Organometallic Catalysis. *Angew. Chem., Int. Ed.* **2013**, *52*, 4744–4788; g) Khusnutdinova, J. R.; Milstein, D. *Angew. Chem., Int. Ed.* **2015**, *54*, 12236–12273. Selected reviews with first row metal-ligand cooperative catalyst : h) van der Vlugt, J. I. Cooperative Catalysis with First-Row Late Transition Metals. *Eur. J. Inorg. Chem.* **2012**, 363–375; i) Elsby, M. R.; Baker, R. T. Strategies and mechanisms of metal–ligand cooperativity in first-row transition metal complex catalysts. *Chem. Soc. Rev.* **2020**, *49*, 8933–8987.
- (2) a) Mum, Y.; Czarkle, D.; Rahamim, Y.; Shvo, Y. (Cyclopentadienone)ruthenium carbonyl complexes - a new class of homogeneous hydrogenation catalysts. *Organometallic* **1985**, *4*, 1459–1461; b) Shvo, Y.; Czarkie, D.; Rahamim, Y.; Chodosh, D. F. A New Group of Ruthenium Complexes: Structure and Catalysis. *J. Am. Chem. Soc.* **1986**, *108*, 7400–7402; c) Menashe, N.; Shvo, Y. Catalytic disproportionation of aldehydes with ruthenium complexes. *Organometallics* **1991**, *10*, 3885–3891; d) Menashe, N.; Salant, E.; Shvo, Y. Efficient catalytic reduction of ketones with formic acid and ruthenium complexes. *J. Organomet. Chem.* **1996**, *514*, 97–102.
- (3) Kumar, P.; Gupta, R K.; Pandey, D. S. Half-sandwich arene ruthenium complexes: synthetic strategies and relevance in catalysis. *Chem. Soc. Rev.* **2014**, *43*, 707–733.
- (4) a) Conley, B. L.; Pennington-Boggio, M. K.; Boz, E.; Williams, T. J. Discovery, Applications, and Catalytic Mechanisms of Shvo’s Catalyst. *Chem. Rev.* **2010**, *110*, 2294–2312; b) Warner, M. C.; Casey, C. P.; Bäckvall, J.-E. Bifunctional Molecular Catalysis. *Topics in Organometallic Chemistry* **2011**, *37*, 85–125.
- (5) a) Gusev, D. G.; Spasyuk, D. M. Revised Mechanisms for Aldehyde Disproportionation and the Related Reactions of the Shvo Catalyst. *ACS Catal.* **2018**, *8*, 6851–6861. b) Dub, P. A.; Gordon, J. C. Metal–Ligand Bifunctional Catalysis: The “Accepted” Mechanism, the Issue of Concertedness, and the Function of the Ligand in Catalytic Cycles Involving Hydrogen Atoms. *ACS Catal.* **2017**, *7*, 6635–6655.
- (6) a) Mays, M. J.; Morris, M. J.; Raithby, P. R.; Shvo Y.; Czarkie D. X-ray structure, reactivity and catalytic properties of a (cyclopentadienone)ruthenium dimer, [(C<sub>4</sub>Ph<sub>4</sub>CO)(CO)<sub>2</sub>Ru]<sub>2</sub>. *Organometallics* **1989**, *8*, 1162–1167. Note that a similar structure was described, see : Casey, C. P.; Singer, S. W.; Powell, D. R.; Hayashi, R. K.; Kavana, M. Hydrogen Transfer to Carbonyls and Imines from a Hydroxycyclopentadienyl Ruthenium Hydride: Evidence for Concerted Hydride and Proton Transfer. *J. Am. Chem. Soc.* **2001**, *123*, 1090–1100.

- (7) van Slagmaat, C. A. M. R.; Delgove, M. A. F.; Stouten, J.; Morick, L.; van der Meer, Y.; Bernaerts, K. V.; De Wildeman, S. M. A. Solvent-free hydrogenation of levulinic acid to  $\gamma$ -valerolactone using a Shvo catalyst precursor: optimization, thermodynamic insights, and life cycle assessment. *Green Chem.* **2020**, *22*, 2443–2458.
- (8) Igau, A.  $\eta^5$ -Oxocyclohexadienyl ligands in transition metal chemistry: Neglected (Brønsted) base ligands in cooperative catalysis. *Coord. Chem. Rev.* **2017**, *344*, 299–322.
- (9) a) Adams, J. R.; Bennett, M. A. Transition Metal Complexes of Tethered Arenes. *Adv. Organomet. Chem.* **2006**, *54*, 293–332; b) Bennett, M. A.; Harper, J. R. in *Modern Coordination Chemistry*, ed. G. J. Leigh and N. Winterton, RSC Publishing, Cambridge, 2002, pp. 163–168 and references cited therein; c) Umezawa-Vizzini, K.; Lee, T. R. Reversible Olefin–Hydride Insertion in the Cationic Ruthenium Complexes  $[(\eta^6\text{-C}_6\text{H}_5\text{CH}_2\text{CH}_2\text{PR}_2)\text{RuH}(\text{CH}_2\text{CH}_2)]^+$ . *Organometallics* **2004**, *23*, 1448–1452; d) Faller, J. W.; Fontaine, P. P. Resolution and Diels–Alder Catalysis with Planar Chiral Arene-Tethered Ruthenium Complexes. *Organometallics* **2005**, *24*, 4132–4138; e) Pinto, P.; Götz, A. W.; Marconi, G.; Hess, B. A.; Marinetti, A.; Heinemann, F. W.; Zenneck, U. Diastereoselective Synthesis of Arene Ruthenium(II) Complexes Containing Chiral Phosphetane-Based Tethers. *Organometallics* **2006**, *25*, 2607–2616; f) Aznar, R.; Grabulosa, A.; Mannu, A.; Muller, G.; Sainz, D.; Moreno, V.; Font-Bardia, M.; Calvet, T.; Lorenzo, J.  $[\text{RuCl}_2((\eta^6\text{-p-cymene})(\text{P}^*))]$  and  $[\text{RuCl}_2(\kappa\text{-P}^*[(\eta^6\text{-arene})])]$  Complexes Containing *P*-Stereogenic Phosphines. Activity in Transfer Hydrogenation and Interactions with DNA. *Organometallics* **2013**, *32*, 2344–2362; g) Ito, M.; Endo, Y.; Ikariya, T. Well-Defined Tri-flylamide-Tethered Arene–Ru(Tsdpen) Complexes for Catalytic Asymmetric Hydrogenation of Ketones. *Organometallics* **2008**, *27*, 6053–6055; h) Parekh, V.; Ramsden, J. A.; Wills, M. Ether-tethered Ru(II)/TsDPEN complexes; synthesis and applications to asymmetric transfer hydrogenation. *Catal. Sci. Technol.* **2012**, *2*, 406–411; i) González-Fernández, R.; Crochet, P.; Cadierno, V. *Dalton Trans.* **2020**, *49*, 210–222.
- (10) Kechaou-Perrot, M.; Vendier, L.; Bastin, S.; Sotiropoulos, J.-M.; Miqueu, K.; Menéndez-Rodríguez, L.; Crochet, P.; Cadierno, V.; Igau, A. Tethered  $\eta^5$ -oxocyclohexadienyl piano-stool ruthenium(II) complexes: A new class of catalysts? *Organometallics* **2014**, *33*, 6294–6297.
- (11) Cole-Hamilton, D. J.; Young, R. J.; Wilkinson G. J.  $\pi$ -Arene and  $\pi$ -Phenoxo Complexes of Ruthenium and Rhodium. *Chem. Soc., Dalton Trans.* **1976**, 1995–2001.
- (12) a) Luca, L. D.; Mezzetti, A. Chiral Benzoin via Asymmetric Transfer Hemihydrogenation of Benzils: The Detail that Matters. *J. Org. Chem.* **2020**, *85*, 5807–5814; b) Luca, L. D.; Mezzetti, A. Base-Free Asymmetric Transfer Hydrogenation of 1,2-Di- and Monoketones Catalyzed by a  $(\text{NH})_2\text{P}_2$ -Macrocyclic Iron(II) Hydride. *Angew. Chem. Int. Ed.* **2017**, 11949–11953; c) Clapham, S. E.; Iuliis, M. Z.-D.; Mack, K.; Prokopchuk, D. E.; Morris, R. H. Alcohol-assisted base-free hydrogenation of acetophenone catalyzed by  $\text{OsH}(\text{NHCMe}_2\text{CMe}_2\text{NH}_2)(\text{PPh}_3)_2$ . *Can. J. Chem.* **2014**, *92*, 731–738; d) He, L. P.; Chen, T.; Xue, D.-X.; Eddaoudi, M.; Huang, K.-W. Efficient transfer hydrogenation reaction Catalyzed by a dearomatized  $\text{PN}^3\text{P}$  ruthenium pincer complex under base-free Conditions. *J. Organomet. Chem.* **2012**, *700*, 202–206; e) Clarke, Z. E.;



- Maragh, P. T.; Dasgupta, T. P.; Gusev, D. G.; Lough, A. J.; Abdur-Rashid, K. A Family of Active Iridium Catalysts for Transfer Hydrogenation of Ketones. *Organometallics* **2006**, *25*, 4113–4117; f) Dong, Z.-R.; Li, Y.-Y.; Chen, J.-S.; Li, B.-Z.; Xing, Y.; Gao, J.-X.; Highly, J.-X. Highly Efficient Iridium Catalyst for Asymmetric Transfer Hydrogenation of Aromatic Ketones under Base-Free Conditions. *Org. Lett.* **2005**, *7*, 1043–1045.
- (13) a) Kalsin, A. M.; Peganova, T. A.; Sinopalnikova, I. S.; Fedyanin, I. V.; Belkova, N. V.; Deydier, E.; Poli, R. Mechanistic diversity in acetophenone transfer hydrogenation catalyzed by ruthenium iminophosphonamide complexes. *Dalton Trans.* **2020**, *49*, 1473–1484; b) Medrano-Castillo, L.-J.; Collazo-Flores, M. A.; Camarena-Díaz, J. P.; Correa-Ayala, E.; Chávez, D.; Grotjahn, D. B.; Rheingold, A. L.; Miranda-Soto, V.; Parra-Hake, M. Base-free transfer hydrogenation of aryl-ketones, alkyl-ketones and alkenones catalyzed by an Ir<sup>III</sup>Cp\* complex bearing a triazenide ligand functionalized with pyrazole. *Inorg. Chim. Acta* **2020**, *507*, 119551; c) Dubey, P.; Gupta, S.; Singh, A. K. Complexes of Pd(II),  $\eta^6$ -C<sub>6</sub>H<sub>6</sub>Ru(II), and  $\eta^5$ -Cp\*Rh(III) with Chalcogenated Schiff Bases of Anthracene-9-carbaldehyde and Base-Free Catalytic Transfer Hydrogenation of Aldehydes/Ketones and N-Alkylation of Amines. *Organometallics* **2019**, *38*, 944–961; d) Satheesh, C. E.; Sathish Kumar, P. N.; Kumara, P. R.; Karvembu, R.; Hosamani, A.; Nethaji, M. Half-sandwich Ru (II) complexes containing (N, O) Schiff base ligands: Catalysts for base-free transfer hydrogenation of ketones. *Appl. Organometal. Chem.* **2019**, *33*, e5111-e5116; e) Roach, T. V.; Schmitz, M. L.; Leach, V. A.; Miller, M. D.; Chan, B. C.; Kalman, S. E. Nickel complexes of primary amido-functionalized *N*-heterocyclic carbene ligands: Synthesis, characterization, and base-free transfer hydrogenation. *J. Organomet. Chem.* **2018**, *873*, 8–14; f) Dubey, P.; Gupta, S.; Singh, A. K. Base free N-alkylation of anilines with ArCH<sub>2</sub>OH and transfer hydrogenation of aldehydes/ketones catalyzed by the complexes of  $\eta^5$ -Cp\*Ir(III) with chalcogenated Schiff bases of anthracene-9-carbaldehyde. *Dalton Trans.* **2018**, *47*, 3764–3774; g) Kerner, C.; Lang, J.; Gaffga, M.; Menges, F. S.; Sun, Y.; Niedner-Schatteburg, G.; Thiel, W. R. Mechanistic Studies on Ruthenium(II)-Catalyzed Base-Free Transfer Hydrogenation Triggered by Roll-Over Cyclometalation. *ChemPlusChem* **2017**, *82*, 212–224; h) Navarro, M.; Smith, C. A.; Albrecht, M. Enhanced Catalytic Activity of Iridium(III) Complexes by Facile Modification of C,N-Bidentate Chelating Pyridylideneamide Ligands. *Inorg. Chem.* **2017**, *56*, 11688–11701; i) Sommer, M. G.; Marinova, S.; Krafft, M. J.; Urankar, D.; Schweinfurth, D.; Bubrin, M.; Košmrlj, J.; Sarkar, B. Ruthenium Azocarboxamide Half-Sandwich Complexes: Influence of the Coordination Mode on the Electronic Structure and Activity in Base-Free Transfer Hydrogenation Catalysis. *Organometallics* **2016**, *35*, 2840–2849; j) Ruff, A.; Kirby, C.; Chan, B. C.; O'Connor, A. R. Base-Free Transfer Hydrogenation of Ketones Using Cp\*Ir(pyridinesulfonamide)Cl Precatalysts. *Organometallics* **2016**, *35*, 327–335; k) Ghoochany, L. T.; Kerner, C.; Farsadpour, S.; Menges, F.; Sun, Y.; Niedner-Schatteburg, G.; Thiel, W. R. C–H Activation at a Ruthenium(II) Complex – The Key Step for a Base-Free Catalytic Transfer Hydrogenation? *Eur. J. Inorg. Chem.* **2013**, 4305–4317; l) Carrión, M. C.; Sepúlveda, F.; Jalón, F. A.; Manzano, B. R.; Rodríguez, A. M. Areneruthenium(II) Complexes Containing Bispyrazolylmethane Ligands: Effect of the Ligand Substituents on the Formation of

- an Isomer and on the Fluxional Behaviour. *Eur. J. Inorg. Chem.* **2013**, 217–227; m) Elliott, A. G.; Green, A. G.; Diaconescu, P. L. Transfer hydrogenation with a ferrocene diamide ruthenium complex. *Dalton Trans.* **2012**, 41, 7852–7854; n) Kumar, M.; DePasquale, J.; White, N. J.; Zeller, M.; Papish, E. T. Ruthenium Complexes of Triazole-Based Scorpionate Ligands Transfer Hydrogen to Substrates under Base-Free Conditions. *Organometallics* **2013**, 32, 2135–2144; o) Carrión, M. C.; Sepúlveda, F.; Jalón, F. A.; Manzano, B. R., Rodríguez, A. M. Base-Free Transfer Hydrogenation of Ketones Using Arene Ruthenium(II) Complexes. *Organometallics* **2009**, 28, 3822–3833; p) Corberán, R.; Peris, E. An Unusual Example of Base-Free Catalyzed Reduction of C=O and C=NR Bonds by Transfer Hydrogenation and Some Useful Implications. *Organometallics* **2008**, 27, 1954–1958; q) Castarlenas, R.; Esteruelas, M. A.; Oñate, E. Preparation, X-ray Structure, and Reactivity of an Osmium-Hydroxo Complex Stabilized by an N-Heterocyclic Carbene Ligand: A Base-Free Catalytic Precursor for Hydrogen Transfer from 2-Propanol to Aldehydes. *Organometallics* **2008**, 27, 3240–3247.
- (14) a) Ohkuma, T.; Utsumi, N.; Tsutsumi, K.; Murata, K.; Sandoval, C.; Noyori, R. The Hydrogenation/Transfer Hydrogenation Network: Asymmetric Hydrogenation of Ketones with Chiral  $\eta^6$ -Arene/N-Tosylethylenediamine–Ruthenium(II) Catalysts. *J. Am. Chem. Soc.* **2006**, 128, 8724–8725; b) Ohkuma, T.; Tsutsumi, K.; Utsumi, N.; Arai, N.; Noyori, R.; Murata, K. Reductive Ring Opening of o-Nitrobenzylidene Acetals of Monosaccharides: Synthesis and Photolysis of Some Photolabile Sugars. *Org. Lett.* **2007**, 9, 255–257.
- (15) Langer, R.; Iron, M. A.; Konstantinovski, L.; Diskin-Posner, Y.; Leitun, G.; Ben-David, Y.; Milstein, D. Iron Borohydride Pincer Complexes for the Efficient Hydrogenation of Ketones under Mild, Base-Free Conditions: Synthesis and Mechanistic Insight. *Chem. Eur. J.* **2012**, 18, 7196–7209.
- (16) a) Jiang, F.; Yuan, K.; Achard, M.; Bruneau, C. Ruthenium-Containing Phosphinesulfonate Chelate for the Hydrogenation of Aryl Ketones. *Chem. Eur. J.* **2013**, 19, 10343–10352; b) Zhang, G.; Vasudevan, K. V.; Scott, B. L.; Hanson, S. K. Understanding the Mechanisms of Cobalt-Catalyzed Hydrogenation and Dehydrogenation Reactions. *J. Am. Chem. Soc.* **2013**, 135, 8668–8681; c) Facchini, S. V.; Neudörfl, J.-M.; Pignataro, L.; Cettolin, M.; Gennari, C.; Berkessel, A.; Piarulli, U. Synthesis of [Bis(hexamethylene) cyclopentadienone]iron Tricarbonyl and its Application to the Catalytic Reduction of C=O Bonds. *ChemCatChem* **2017**, 9, 1461–1468; d) Yao, Z.-J.; Zhu, J.-W.; Lin, N.; Qiao, X.-C.; Deng, W. Catalytic hydrogenation of carbonyl and nitro compounds using an [N,O]-chelate half-sandwich ruthenium catalyst. *Dalton Trans.* **2019**, 48, 7158–7166; e) Wang, R.; Qi, J.; Yue, Y.; Lian, Z.; Xiao, H.; Zhuo, S.; Xing, L. Ambient-pressure hydrogenation of ketones and aldehydes by a metal-ligand bifunctional catalyst [Cp\*Ir(2,2'-bpyO)(H<sub>2</sub>O)] without using base. *Tetrahedron* **2019**, 75, 130463.
- (17) Watanabe, Y.; Ohta, T.; Tsuji, Y. Ruthenium-catalyzed Reduction of Carbonyl Compounds Using Formic Acid. *Bull. Chem. Soc. Jpn* **1982**, 55, 2441–2444.

- (18) Wu, W.; Seki, T.; Walker, K. L.; Waymouth, R. M. Transfer Hydrogenation of Aldehydes, Allylic Alcohols, Ketones, and Imines Using Molybdenum Cyclopentadienone Complexes. *Organometallics* **2018**, *37*, 1428–1431.
- (19) Murayama, H.; Heike, Y.; Higashida, K.; Shimizu, Y.; Yodsin, N.; Wongnongwa, Y.; Jungstittiwong, S.; Mori, S.; Sawamura, M. Iridium-Catalyzed Enantioselective Transfer Hydrogenation of Ketones Controlled by Alcohol Hydrogen-Bonding and sp<sup>3</sup>-C–H Noncovalent Interactions. *Adv. Synth. Catal.* **2020**, *362*, 1–8.
- (20) Yuki, Y.; Touge, T.; Nara, H.; Matsumura, K.; Fujiwhara, M.; Kayaki, Y.; Ikariya, Y. Selective Asymmetric Transfer Hydrogenation of  $\alpha$ -Substituted Acetophenones with Bifunctional Oxo-Tethered Ruthenium(II) Catalysts. *Adv. Synth. Catal.* **2018**, *360*, 568-574.
- (21) a) Deng, J.; Wang, J.; Pan, T.; Xu, Q.; Guo, Q-X.; Fu, Y. Conversion of carbohydrate biomass to  $\gamma$ -valerolactone by using water-soluble and reusable iridium complexes in acidic aqueous media. *ChemSusChem* **2013**, *6*, 1163-1167; b) Fabos, V.; Mika, L. T.; Horvath, I. T. Selective Conversion of Levulinic and Formic Acids to  $\gamma$ -Valerolactone with the Shvo Catalyst. *Organometallics* **2014**, *33*, 181-187; c) Wang, S.; Huang, H.; Dorcet, V.; Bruneau, C.; Fischmeister, C. Efficient Iridium Catalysts for Base-Free Hydrogenation of Levulinic Acid. *Organometallics* **2017**, *36*, 3151-3162; d) van Slagmat, C. A. M. R.; De Wildeman, S. M. A. A Comparative Study of Structurally Related Homogeneous Ruthenium and Iron Catalysts for the Hydrogenation of Levulinic Acid to  $\gamma$ -Valerolactone. *Eur. J. Inorg. Chem.* **2018**, 694-702; e) Liu, Z.; Yang, Z.; Wang, P.; Yu, X.; Wu, Y.; Wang, H.; Liu, Z. Co-catalyzed Hydrogenation of Levulinic Acid to  $\gamma$ -Valerolactone under Atmospheric Pressure. *ACS. Sust. Chem. Eng.* **2019**, *7*, 18236-18241; f) van Slagmat, C. A. M.R.; Delgove, M. A. F.; Stouten, J.; Morick, L.; van der Meer, Y.; Bernaerts, K. V.; De Wildeman, S. M. A. Solvent-free hydrogenation of levulinic acid to  $\gamma$ -valerolactone using a Shvo catalyst precursor: optimization, thermodynamic insights, and life cycle assessment. *Green Chem.* **2020**, *22*, 2443-2458.
- (22) Liu, X.; Li, S.-S.; Liu, Y.-M.; Cao, Y. Formic acid: A versatile renewable reagent for green and sustainable chemical synthesis. *Chin. J. Catal.* **2015**, *36*, 1461–1475.
- (23) The influence of the solvent when FA is used as an hydrogen donor in catalysis has been largely reported in the literature, see examples : a) Wienhöfer, G.; Sorribes, I.; Boddien, A.; Westerhaus, F.; Junge, K.; Llusar, R.; Beller, M. General and Selective Iron-Catalyzed Transfer Hydrogenation of Nitroarenes without Base. *J. Am. Chem. Soc.* **2011**, *133*, 12875–12879. b) Zhao, B.; Hu, Y.; Gao, J.; Zhao, G.; Ray, M. B.; Xu, C. C. Recent Advances in Hydroliquefaction of Biomass for Bio-oil Production Using In Situ Hydrogen Donors. *Ind. Eng. Chem. Res.* **2020**, *59*, 16987–17007.
- (24) Kechaou-Perrot, M. ; Vendier, L. ; Igau, A. Chlorido( $\eta^6$ - $N^2$ -diphenylphosphanyl- $N^1, N^1$ -diisopropyl-4-methoxybenzamidine- $\kappa P$ )(triphenylphosphane- $\kappa P$ )-ruthenium(II) trifluoromethanesulfonate acetone disolvate *Acta Cryst.* **2013**, *E69*, m659–m660.
- (25) When hydrogen bonding interaction occurs with the oxygen atom, the C–O bond length is elongated and ranges from 1.25 to 1.29 Å.

- (26) Soleimannejad J., Colin White C. A Convenient One-Pot Synthesis of a Functionalized-Arene Ruthenium Half-Sandwich Compound  $[\text{RuCl}_2(\eta^6\text{-C}_6\text{H}_5\text{OCH}_2\text{CH}_2\text{OH})_2]$ . *Organometallics* **2005**, *24*, 2538-2541 and references cited therein.
- (27) a) Therrien, B.; Ward, T. R. Synthesis of a Configurationally Stable Three-Legged Piano-Stool Complex. *Angew. Chem., Int. Ed.* **1999**, *38*, 405–408. b) Faller, J. W.; D'Alliessi, D. G. Planar Chirality in Tethered  $\eta^6$ :  $\eta^1$ - (Phosphinophenylenearene-*P*)ruthenium(II) Complexes and Their Potential Use as Asymmetric Catalysts. *Organometallics* **2003**, *22*, 2749–2757. c) Cetinkaya, B.; Demir, S.; Ozdemir, I.; Toupet, L.; Sémeril, D.; Bruneau, C.; Dixneuf, P. H.  $\eta^6$ -Mesityl,  $\eta^1$ -Imidazolinylidene–Carbene–Ruthenium(II) Complexes: Catalytic Activity of their Allenylidene Derivatives in Alkene Metathesis and Cycloisomerisation Reactions. *Chem. Eur. J.* **2003**, *9*, 2323–2330. d) Cadierno, V.; Díez, J.; García-Álvarez, J.; Gimeno, J. A new class of tethered-arene ruthenium(II) complexes with pendant P and C donor atoms: synthesis of  $\eta^6$ :  $\eta^1$ :  $\eta^1$  phosphonio-azabutadienyl ruthenabicycles via allenylidene intermediates. *Chem. Commun.* **2004**, 1820–1821.
- (28) a) Kalutharage, N. ; Yi, C. S. Scope and Mechanistic Analysis for Chemoselective Hydrogenolysis of Carbonyl Compounds Catalyzed by a Cationic Ruthenium Hydride Complex with a Tunable Phenol Ligand. *J. Am. Chem. Soc.* **2015**, *137*, 11105–11114. b) Snelgrove, J. L. ; Conrad, J. C. ; Yap, G. P. A. ; Fogg, D. E. The kinetic instability of  $\sigma$ -bound aryloxide in coordinatively unsaturated or labile complexes of ruthenium. *Inorg. Chim. Acta* **2003**, *345*, 268–278.
- (29) a) Lastra-Barreira, B. ; Díez, J. ; Crochet, P. ; Fernández, I. Functionalized arene–ruthenium(II) complexes: dangling vs. tethering side chain. *Dalton Trans.*, **2013**, *42*, 5412–5420; b) Lastra-Barreira, B.; Díez, J.; Crochet, P. Highly water-soluble arene-ruthenium(II) complexes: application to catalytic isomerization of allylic alcohols in aqueous medium. *Green Chem.* **2009**, *11*, 1681-1686. c) Lastra-Barreira, B.; Crochet, P. *Green Chem.* **2010**, *12*, 1311-1314.
- (30) a) Akhbari, K.; Morsali, A. Halogen dipole moment effect of phenolic ring on formation of stair like polymers or polymers with tetranuclear cubic cage units; new precursors for preparation of  $\text{TlCl}$  and  $\text{Tl}_2\text{O}_3$  nanostructures. *CrystEngCom* **2012**, *14*, 1618–1628 ; b) Roesky, H. W. ; Scholz, M. ; Noltemeyer, M. ; Edelmann, F. T. Preparation and crystal structure of thallium 2,4,6-tris(trifluoromethyl)phenoxide, a compound of thallium(I) with coordination number 2 at the thallium atom. *Inorg. Chem.* **1989**, *28*, 3829-3830.
- (31) Arquier, D. ; Vendier, L. ; Miqueu, K. ; Sotiropoulos, J.-M. ; Bastin, S. ; Igau, A. Crucial Role of the Amidine Moiety in Methylenamino Phosphine-Type Ligands for the Synthesis of Tethered  $\eta^6$ -Arene-  $\eta^1$ -P Ruthenium(II) Complexes: Experimental and Theoretical Studies. *Organometallics* **2009**, *28*, 4945–4957.
- (32) a) Ganguli, K. ; Shee, S. ; Panja, D. ; Kundu, S. Cooperative Mn(I)-complex catalyzed transfer hydrogenation of ketones and imines. *Dalton Trans.* **2019**, *48*, 7358-7366; b) Wei, D. ; Bruneau-Voisine, A. ; Dubois, M. ; Bastin, S. ; Sortais, J.-B. Manganese-Catalyzed Transfer Hydrogenation of Aldimines. *ChemCatChem* **2019**, *11*, 5256-5259; c) Bauri, S. ; Donthireddy, S. N. R. ; Mathoor Ilan, P. ; Rit, A. Effect of Ancillary Ligand in Cyclometalated Ru(II)–NHC-Catalyzed Transfer Hydrogenation of Unsaturated Compounds. *Inorg. Chem.*

**2018**, 57, 14582-14593; d) Wang, C.; Pettman, A.; Basca, J; Xiao, .J. A Versatile Catalyst for Reductive Amination by Transfer Hydrogenation. *Angew. Chem. Int. Ed.* **2010**, 49, 7548-7552.

- (33) In view of the theoretical studies lately reported in the catalytic ketone reduction with metal-ligand cooperative catalysts which have revisited long-standing “accepted“ mechanism, further experimental work and computations need to be investigated to have a reliable mechanistic insight for our catalytic system.